Polymer Chemistry

PAPER

All-acrylic superelastomers: facile synthesis and exceptional mechanical behavior†

Cite this: DOI: 10.1039/c7py01518f

Wei Lu,[a] Andrew Goodwin,[a] Yangyang Wang,[b] Panchao Yin,[c] Weiyu Wang,[b] Jiahua Zhu,[b] Ting Wu,[d] Xinyi Lu,[a] Bin Hu,[d] Kunlun Hong,*[b] Nam-Goo Kang*[a] and Jimmy Mays*[a]

Received 5th September 2017,
Accepted 12th October 2017

DOI: 10.1039/c7py01518f

rsc.li/polymers

All-acrylic multigraft copolymers, poly(butyl acrylate)-*g*-poly(methyl methacrylate), synthesized using a facile grafting-through methodology, exhibit elongation at break (>1700%) and strain recovery behavior far exceeding those of any commercial acrylic (~500%) and styrenic (~1000%) triblock copolymers to date. One-batch anionic polymerization of methyl methacrylate (MMA) using the *sec*-butyl lithium/*N*-isopropyl-4-vinylbenzylamine (*sec*-BuLi/PVBA) initiation system gives PMMA macromonomers with quantitative yield, short reaction time, and using simple synthetic procedures. These new all-acrylic superelastomers and the simple synthetic approach greatly expand the range of potential applications of all-acrylic thermoplastic elastomers (TPEs).

Introduction

Thermoplastic elastomers (TPEs) have been widely used in industry in applications such as shape memory, adhesives, footwear, food packaging and road surface dressings.[1–3] When compared to the more widely used styrenic TPEs, all-acrylic TPEs offer great potential to address issues with styrenic TPEs such as limited upper service temperature[4–6] and susceptibility to oxidation and photolysis.[7] However, their much higher molecular weight between chain entanglements (M_e) leads to much poorer mechanical strength, elongation at break and elastic recovery of all-acrylic TPEs as compared to styrenic TPEs.[8–10] Improvements in elongation at break while maintaining high tensile strength are desirable to improve the performance in many applications, such as gloves, condoms, and even simple items like rubber bands. With increased elongation at break and high elastic recovery, the materials can be made using less elastomer (reduced cost and weight) and thus be made thinner.[8] This offers advantages of cost saving and product improvements, such as thinner surgical gloves and condoms.

The use of complex macromolecular architectures offers a potential approach to address this issue. As compared to linear block copolymers, polymers with complex architectures can exhibit superior physical and mechanical properties.[11] Furthermore, block copolymers having miktoarm stars or graft/multigraft architectures provide additional capacity to tune the morphology and thus the modulus of the TPE.[12–14] We have previously reported a multigraft copolymer composed of polyisoprene (PI) as the backbone and polystyrene (PS) as the side chains, which were termed "superelastomers", due to their 1500% or greater elongation at break, far exceeding that of commercial polystyrene-*b*-polyisoprene-*b*-polystyrene (SIS) triblock copolymers with strain at break around 1000%.[15–18]

Multigraft copolymers are normally synthesized through three strategies: grafting onto, grafting from and grafting through (macromonomer approach).[19] Among these approaches, the "grafting through" methodology provides a better capacity to produce graft copolymers with side chains having a fixed length.[20] All-acrylic multigraft copolymers, *e.g.* poly(*n*-butyl acrylate)-*g*-poly(methyl methacrylate) (PBA-*g*-PMMA), have been exploited with good strain at break (>400%) and tunable tensile strength.[21–23] The PMMA macromonomer has been synthesized by anionic polymerization using 1-(*tert*-butyldimethylsiloxy)-3-butyllithium as a protected initiator, followed by deprotection and conversion to the PMMA macromonomer (MM-PMMA). The macromonomer has also been synthesized through the coupling reaction with 4-vinylbenzyl chloride.[24] However, both of these previously reported routes involve linking reactions or post-polymerization modification reactions that have limitations, including complex operation, low conversion and long reaction times.

[a]Department of Chemistry, University of Tennessee, Knoxville, Tennessee 37996, USA. E-mail: nkang1@utk.edu, jimmymays@utk.edu
[b]Center for Nanophase Materials Sciences, Oak Ridge National Laboratory, Oak Ridge, Tennessee 37831, USA. E-mail: hongkq@ornl.gov
[c]Chemical and Engineering Materials Division, Oak Ridge National Laboratory, Oak Ridge, Tennessee 37831, USA
[d]Department of Materials Science and Engineering, University of Tennessee, Knoxville, Tennessee 37996, USA

†Electronic supplementary information (ESI) available. See DOI: 10.1039/c7py01518f

In this work, we report a facile approach to synthesize PBA-*g*-PMMA by using a grafting through methodology. The PMMA macromonomer was produced by anionic polymerization directly in one batch using *N*-isopropyl-4-vinylbenzylamine (PVBA) as the initiator. As previously reported, the reactivity gap between the carbanion and nitranion can give rise to the polymerization of methacrylate groups, with styrenic vinyl groups remaining intact.[25] Thus the synthesis of the macromonomer can be achieved in a one-batch reaction with 100% conversion and short reaction time, taking advantage of the "living" nature of anionic polymerization.[26,27] The final PBA-*g*-PMMA graft copolymer was synthesized by reversible addition–fragmentation chain-transfer (RAFT) polymerization. The resulting graft copolymer was characterized using nuclear magnetic resonance (NMR) spectroscopy and size exclusion chromatography (SEC) for molecular information. Differential scanning calorimetry (DSC) was used to characterize the thermal properties of the materials. The microphase separation behaviors were investigated using atomic force microscopy (AFM) and small angle X-ray scattering (SAXS). In addition, the mechanical properties of the graft copolymers were studied using dynamic mechanical analysis (DMA) and uniaxial tensile tests.

Experimental

Materials

Isopropylamine (Acros Organics, 99%), 4-vinylbenzyl chloride (Acros Organics, 90%), *sec*-butyllithium (*sec*-BuLi), 1,1-diphenyl ethylene (DPE, Acros Organics, 98%), tetrahydrofuran (THF) (Fisher, GR grade) and methanol (Fisher, GR grade) were prepared and purified as previously described.[27] LiCl (Alfa Aesar, 99.995%) was dried at 130 °C for 2 days and ampulized under high vacuum conditions. Methyl methacrylate (MMA, Aldrich, 99%) was passed through an aluminum oxide (Acros Organics, basic) column to remove the inhibitor, stirred for 24 h over anhydrous CaH_2 and distilled over calcium hydride (CaH_2) and trioctylaluminum sequentially under reduced pressure. The resulting MMA was ampulized and diluted immediately with THF under high vacuum conditions, giving a concentration of 0.8–0.9 mmol mL^{-1}. All ampules of the reactants equipped with break seals were stored at −30 °C.

N-Butyl acrylate (BA, Acros Organics, 99%) was used directly after passing through an aluminum oxide (Acros Organics, basic) column to remove the inhibitor. 2,2-Azobis-(isobutyronitrile) (AIBN, Sigma-Aldrich, 90%) was recrystallized from methanol before use and the *S*-1-dodecyl-*S*′-(α,α′-dimethyl-α′-acetic acid) trithiocarbonate chain transfer agent (CTA) was synthesized following the procedure previously published by Lai *et al.*[28] Benzene (Aldrich, ≥99.9%), sodium hydroxide (NaOH, Acros Organics, 98%), magnesium sulfate ($MgSO_4$, Aldrich, 99.5%), and sodium chloride (NaCl, Acros Organics, 99.5%) were used as received.

Synthesis of *N*-isopropyl-4-vinylbenzylamine (PVBA)

PVBA was synthesized following the previously reported work.[29] Briefly, the procedure was as follows: the reaction was carried out under an atmosphere of nitrogen. A 250 mL round bottom flask with 4-vinylbenzyl chloride (10 g, 65.5 mmol) was cooled to 0 °C with an ice bath. Isopropylamine (15.5 g, 262.2 mol) was added to the flask. The reaction solution was heated to room temperature and left stirring for 24 h. After the reaction was complete, the solution was diluted with dichloromethane, and extracted with saturated aqueous NaOH solution, saturated aqueous NaCl solution and deionized water (DIO) sequentially. The combined organic layers were dried over anhydrous $MgSO_4$, evaporated, and purified using a flash column with hexane as the eluant. A light orange oil-like liquid was obtained after the evaporation of hexane. The resulting product was obtained with the yield of 73%. ^{1}H NMR spectra ($CDCl_3$, 500 MHz), δ (ppm): 7.31 and 7.37 (d, 4H, –Ar), 6.74 (dd, 1H, C═CH–Ar), 5.72 and 5.24 (dd, 2H, CH_2═C–Ar), 3.76 (s, 2H, N–CH_2–Ar), 2.83 (sept, 1H, N–CH–C_2), 1.09 (d, 6H, CH_3–C–N).

For anionic polymerization, PVBA was further stirred over CaH_2 overnight, and distilled into an ampule equipped with a break-seal under high vacuum conditions. The purified colorless liquid was diluted with anhydrous THF. The solutions (0.5 mmol mL^{-1} and 0.05 mmol mL^{-1}) were stored at −30 °C until polymerization.

Homopolymerization of PMMA macromonomer

All anionic polymerizations were carried out under high-vacuum conditions (10^{-6} mmHg) in glass apparatus equipped with break-seals in the usual manner.[26,27] The polymerization was performed in THF at −78 °C. The initiation system was prepared by the anion exchange reaction between *sec*-BuLi and PVBA at −78 °C for 30 min. LiCl and MMA were introduced sequentially *via* break-seals. Polymerization was performed for 1 h and terminated with degassed methanol at −78 °C. The product was poured into a large excess of hexane with vigorous stirring. The precipitated polymer was filtered and vacuum-dried overnight. The resulting polymer was characterized by SEC. The intact vinyl group was confirmed by ^{1}H NMR spectroscopy.

Synthesis of PBA-*g*-PMMA graft copolymer

All the PBA-*g*-PMMA graft copolymers were polymerized through reversible addition–fragmentation chain transfer (RAFT) polymerization under high-vacuum conditions (10^{-6} mmHg) in glass apparatus. PMMA macromonomer, CTA, and AIBN were mixed and dissolved in a vial. The solution was transferred to a round bottom flask, which was degassed by three freeze–thaw–evacuate cycles. The flask was flame-sealed under vacuum and immersed in an oil bath at 80 °C for a certain time, depending on different target molecular weights. The polymerization was quenched with liquid nitrogen. The product solution was precipitated in a large excess of methanol with vigorous stirring and vacuum dried overnight. The resulting polymer was characterized by SEC. The ratio of PMMA to PBA was investigated by ^{1}H NMR.

Chemical and thermal property characterization

The molecular weights (MWs) of the polymers were characterized by size exclusion chromatography (SEC) in THF at 40 °C with a flow rate of 1.0 mL min^{-1} using a Polymer Laboratories PL-120 SEC system equipped with four detectors consisting of a Polymer Laboratories refractometer, a Precision Detector PD 2040 (2-angle static light scattering detector), a Precision Detector PD2000DLS (2-angle light scattering detector), and a Viscotek 220 differential viscometer. The column set employed consisted of Polymer Laboratories PLgel; 7.5 × 300 mm; 10 μm; 500, 1×10^4, 1×10^6, and 1×10^7 Å. The ^{1}H NMR spectra were recorded with a Varian VNMR 500 MHz, and using $CDCl_3$ as the solvent. Chemical shifts referred to the $CDCl_3$ solvent peak at 7.26 ppm. Thermal properties were characterized by differential scanning calorimetry (DSC, TA2000) under nitrogen with a heating rate of 10 °C min^{-1}.

Microphase separation behavior characterization

Morphological measurements were performed using atomic force microscopy (AFM) and small-angle X-ray scattering (SAXS).

To prepare samples for AFM measurements, a solution of 50 mg of polymer in 1.0 mL of toluene was stirred overnight at room temperature. Silicon wafers were cleaned by soaking in deionized water, acetone, and isopropanol for one hour in each solvent. Then, the polymer solution was spin-cast on the silicon wafer (1500 rpm for 30 s and 300 rpm for another 30 s). The resulting thin films were dried and annealed at 160 °C for 7 days prior to the measurement. AFM images were collected using an Asylum Research MFP3D with a multimode controller at room temperature in tapping mode with an Al reflex coated Si tip (radius 9 ± 2 nm) at a line scanning frequency of 1 Hz.

Samples for SAXS were prepared as follows: a solution of 50 mg of polymer in 1 mL of toluene was stirred overnight at room temperature and cast into a 1 mL PTFE Griffin beaker and evaporated slowly over 7 days, resulting in films with the thicknesses of around 0.5 mm. All dried samples were annealed at 160 °C for 7 days under vacuum (10^{-6} mmHg) before measurements. SAXS/WAXS experiments were conducted at 12-ID-B at the Advanced Photon Source at Argonne National Laboratory. X-rays of wavelength λ = 0.89 Å were used, and each measurement was performed at two different sample-to-detector distances to cover a q-range of $0.0026 < q < 4.4$ Å^{-1}, where $q = \left(\frac{4\pi}{\lambda}\right)\sin(\theta/2)$ is the magnitude of the scattering vector, and θ is the scattering angle.

Measurement of mechanical properties

The characterization of mechanical properties of polymers included dynamic mechanical analysis (DMA) and uniaxial tensile tests. The samples tested were prepared as follows: a solution of 2.0 g of polymer in 20 ml of toluene was stirred overnight at room temperature and cast into a 25 ml PTFE evaporating dish and evaporated slowly over 7 days, resulting in films with the thicknesses of around 0.5 mm. Then the samples were dried for 2 days in a vacuum oven at around 50 °C. The resulting films were cut into uniform dog-bone shaped specimens (ISO 37-4).

Dynamic mechanical analysis was performed on a TA Instruments Q-800 dynamic mechanical analyzer equipped with a single cantilever clamp. The temperature ramp/frequency sweep experiments were run at 1 Hz over a temperature range of −60 to +140 °C. Uniaxial tensile tests were carried out using Instron 4465 with a cross-head velocity of 50 mm min^{-1}. For each polymer sample, three identical specimens were tested.

Evaluation of the linear viscoelastic properties

Small amplitude oscillatory shear measurements of the branched copolymers were performed on a Hybrid Rheometer 2 (from TA Instruments) with 3 mm parallel plates in the temperature range −45–150 °C. The temperature was controlled by using an Environmental Test Chamber with nitrogen as the gas source.

Results and discussion

Synthesis of PVBA–PMMA macromonomer

Through the initiation system of *sec*-BuLi/PVBA, the PMMA macromonomers were synthesized by anionic polymerization directly in one batch with no post-polymerization modification (Scheme 1a).

PVBA was synthesized by the alkylation of isopropylamine by 4-vinylbenzyl chloride. The anionic polymerization was performed by the sequential addition of PVBA, *sec*-BuLi, LiCl and MMA monomer, and terminated with degassed methanol. The mixing of PVBA and *sec*-BuLi led to the formation of a greenish yellow color (Fig. S1(a)†), which changed to a light orange color after the reaction for 30 min (Fig. S1(b)†). Otherwise, when PVBA was added to the *sec*-BuLi solution, a deep orange color was observed due to the attack of extra *sec*-BuLi to the vinyl group of PBVA. The initiator solution was stable at elevated temperature and was left at room temperature for around 10 min for the removal of possible remaining *sec*-BuLi by its reaction with THF at room temperature.[30] A large excess of LiCl was added to the initiator solution before the addition of MMA at −78 °C to coordinate with the nitrogen anion and suppress the backbiting reactions during the polymerization.[31]

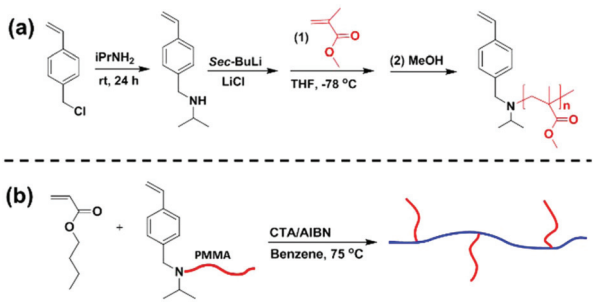

Scheme 1 Synthesis of PBA-*g*-PMMA graft copolymer.

The color change from light orange to blue indicated the formation of a complex between the LiCl salt and the nitrogen anion (Fig. S1(c)†). The solution became colorless once MMA was added, which was the typical phenomenon for living polymethacrylates (Fig. S1(d)†). The intact vinyl group of the resulting macromonomer was confirmed by the ^{1}H NMR spectra, with the chemical shifts at 6.7, 5.8, and 5.2 ppm (Fig. 1a).

Detailed polymerization conditions and molecular weight information are shown in Table 1. The number average molecular weights of the resulting macromonomers were always higher than the calculated values, which might be caused by the trace amount of impurities existing in PVBA ampules, since it was only distilled once over CaH_2 during the ampulization. Still, all the polymers synthesized had a quantitative yield and exhibited a very narrow PDI, which indicated the typical characteristics of anionic polymerization.

Synthesis of PBA-*g*-PMMA graft copolymers

The final PBA-*g*-PMMA graft copolymers were synthesized by reversible addition fragmentation chain-transfer (RAFT) polymerization of BA with the PMMA macromonomer (Scheme 1b). The composition of each graft copolymer was calculated based on the ratio of integrated areas between the peaks at around 3.6 ppm (–OCH_3 of PMMA) and 4.0 ppm (–O–CH_2– of PBA) in ^{1}H NMR spectra (Fig. 1a). The typical SEC curves of the PMMA macromonomer and resulting PBA-*g*-PMMA are shown in Fig. 1b. Detailed molecular weight information is shown in Table 2.

In order to avoid chain transfer to the polymer in conventional free radical polymerizations at high conversions, which could produce unexpected large molecular weight and gelation, and reduce the solubility and processability of the products, the all-acrylic multigraft copolymers of PBA-*g*-PMMA were thus synthesized by reversible addition fragmentation chain-transfer (RAFT) polymerization (Scheme 1b). The reactive ratios for styrene and butyl acrylate in radical copolymerization are 1.00 and 0.23, which indicates that styrene would be a more reactive monomer.[32] However, the connection to a long PMMA polymer chain greatly decreases the reactivity of the styrenic vinyl group due to the steric hindrance. As fully discussed in our previous work with similar multigraft copolymers bearing a styrene end-capped macromonomer, the macromonomers can be randomly distributed in the final graft copolymers.[21,24]

RAFT copolymerizations incorporating high molecular weighted (MW) macromonomers give higher polydispersity indices (PDIs) than conventional RAFT polymerization or copolymerization of low MW monomers because each macromonomer incorporation has a large effect on the overall molecular weight of that particular copolymer chain. Thus chains that incorporate fewer macromonomers will be much lower in MW than those chains that incorporate more macromonomers, broadening the PDI.[21] Even in living anionic copo-

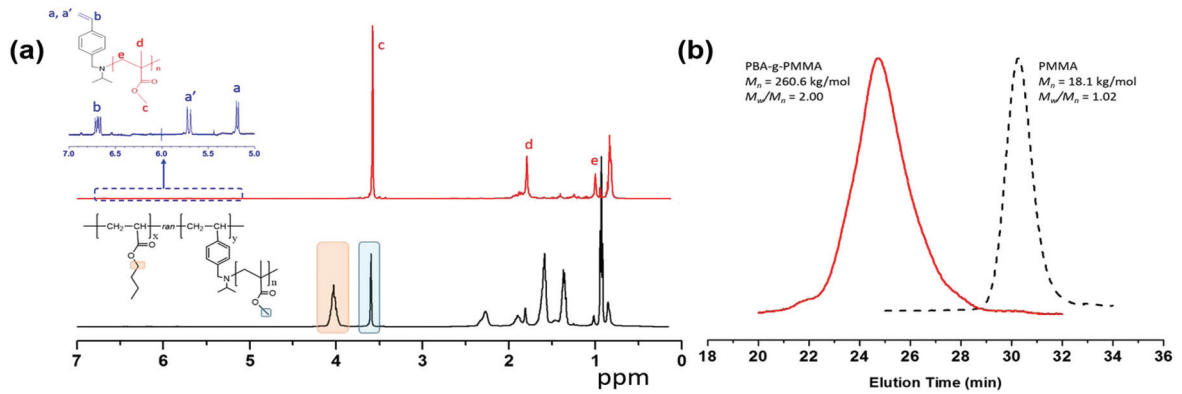

Fig. 1 (a) ^{1}H NMR spectra of PMMA macromonomer (PMMA-18 in Table 1) and PBA-*g*-PMMA (MG-18.1-2.8-18.4 in Table 2); (b) SEC profiles of PBA-*g*-PMMA (MG-18.1-2.8-18.4 in Table 2) and PMMA macromonomer (PMMA-18 in Table 1).

Table 1 Synthesis of PMMA macromonomer by living anionic polymerization[a]

Sample ID	*sec*-BuLi (mmol)	PVBA (mmol)	LiCl (mmol)	MMA (mmol)	Time (min)	M_n (kg mol^{-1}) calcd[c]	M_n (kg mol^{-1}) obsd	M_w/M_n[b]
PMMA-8	0.92	1.50	10.20	30.0	60	3.3	8.4	1.04
PMMA-18	0.80	1.00	10.00	50.0	60	6.3	18.1	1.02
PMMA-29	0.12	0.2	0.1	25.0	60	20.8	29.3	1.01

[a] All the polymerizations showed quantitative yields. [b] Number-average molecular weight M_n and PDI were measured in THF at 40 °C using the Polymer Laboratories PL-120 SEC system, with d*n*/d*c* as 0.085 mL g^{-1} for PMMA. [c] M_n (calcd) = [MMA]/[*sec*-BuLi] × MW(MMA) × yield of polymerization (%).

Table 2 Molecular characteristics and mechanical properties of PBA-*g*-PMMA graft copolymer

	PMMA[b]		PBA-*g*-PMMA[b]							
Sample ID[a]	M_n (kg mol^{-1})	PDI	M_n (kg mol^{-1})	PDI	Conversion[f] (%)	Vol% of PMMA[c]	No.[d]	E[e]	σ_B[e] (MPa)	ε_B[e] (%)
MG-8.4-3.3-8.6	8.4	1.04	294.9	1.99	87.1	8.6	3.3	0.2	1.9	1881
MG-18.1-2.8-18.4	18.1	1.02	260.6	2.00	69.6	18.4	2.8	1.3	4.3	856
MG-29.3-3.0-33.8	29.3	1.01	245.8	1.25	36.5	33.8	3.0	21.9	10.8	497
MG-29.3-1.5-9.3	29.3	1.01	432.6	1.69	49.1	9.3	1.5	0.2	2.0	1712

[a] Sample identification MG-M_n(PMMA)-no. of branch points-vol% of PMMA. [b] Number-average molecular weight M_n and PDI were measured in THF at 40 °C using the Polymer Laboratories PL-120 GPC system, with dn/dc estimated by wt% (PMMA) × 0.085 + wt% (PBA) × 0.067 where 0.085 mL g^{-1} is dn/dc for PMMA and 0.067 is the dn/dc for PBA, and the wt% of PMMA and PBA was obtained from ^{1}H NMR spectra. [c] Vol% was calculated based on the density of 1.159 g mL^{-1} for PMMA and 1.080 g mL^{-1} for PBA. [d] No. of branch points was calculated based on M_n(PBA-*g*-PMMA) × wt% (PMMA)/M_n(PMMA). [e] Young's modulus (E), elongation at break (ε_B) and stress at break (σ_B) were characterized through uniaxial tensile tests. [f] Conversion% was calculated based on M_n(PBA-*g*-PMMA) − (M_n(PMMA) × No.) × mol(CTA)/m(BA).

lymerization involving a normal small monomer and a high molecular weight macromonomer PDIs are much higher than those in normal living anionic polymerizations because of the large effect on MW caused by the incorporation of a single macromonomer.[33,34] The broad PDI contributes to poor order distribution of the morphologies formed by microphase separation. However, as previously discussed in our work on PI-*g*-PS multigraft superelastomers, a well-ordered morphology is not necessary in order to achieve superelasticity for multigraft TPEs.[17]

Thermal properties of PBA-*g*-PMMA graft copolymers

The thermodynamic incompatibility of PBA and PMMA gives rise to their microphase separation. In differential scanning calorimetry (DSC) (Fig. 2a) of MG-18.1-2.8-18.4, both glass transition temperatures (T_gs) at −46 °C and 118 °C were observed, which corresponded to those of PBA and PMMA, respectively. The two glass transitions are also distinctively observed in dynamic mechanical analysis (DMA) (Fig. 2b). A low temperature relaxation process is observed at −43 °C, corresponding to the glass-to-rubber transition of the PBA phase as indicated by a stepwise decrease in storage modulus ($G'(T)$). Further heating led to another drop of $G'(T)$ when the temperature approached 100 °C, corresponding to the glass-to-rubber transition of the PMMA hard phase. The observations of typical T_gs of each domain and the two-step transitions also give a circumstantial indication of the phase separation behavior in the graft copolymers.

Microphase separation behaviors of PBA-*g*-PMMA graft copolymers

Microphase separation behavior of the PBA-*g*-PMMA samples was further investigated using atomic force microscopy (AFM) and small angle X-ray scattering (SAXS).

In the case of AFM images, the bright regions of the phase image represent the stiff domains, *i.e.* PMMA, due to the increase in the phase angle of the probe oscillation. The dark zones represent the soft domains, *i.e.* PBA.[35] Different morphologies were observed with different branch sizes and volume ratios of PMMA, as shown in Fig. 3a and Fig. S2.† With the increase in the chain length of PMMA, the microphase separation behavior was improved. This observation agrees with simulated results by the combination of self-consistent field theory (SCF) and molecular dynamics (MD) simulation proposed by Bates *et al.*, which indicated that the increase in chain length N can promote the phase separation behavior.[36] For this study, longer PMMA chains led to more entanglements between hard domains. Thus a higher degree of phase

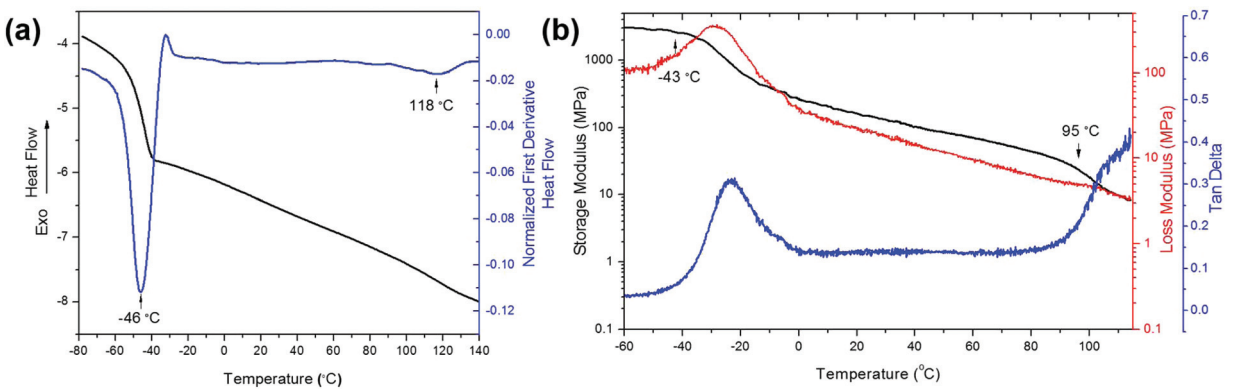

Fig. 2 (a) DSC thermograph of MG-18.1-2.8-18.4 and its normalized first derivative. (b) Storage modulus, loss modulus, and tan δ of MG-18.1-2.8-18.4. Two transitions corresponding to each of the acrylic domains are observed.

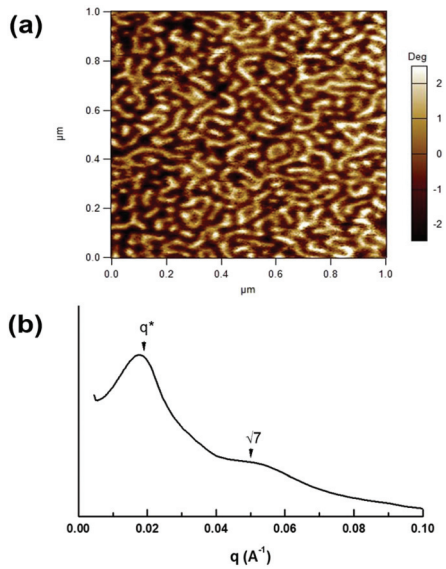

Fig. 3 (a) AFM phase images and (b) SAXS profile of MG-29.3-3.0-33.8.

separation can be achieved. SAXS profiles also exhibit distinctive peaks, reflecting the microphase separation behavior. The broad polydispersity indices contributed to a poor long order distribution of the morphologies. In addition, considering that the graft copolymers are constituted of miktoarm stars, Milner's theory was used to explain this phenomenon.[37] The very high molecular weight and the presence of multiple branch points hinder the ability of the chains to reach equilibrium morphologies, thus, the well-ordered morphology is compromised for graft copolymers, even with a well-controlled structure, including regular spacing and narrow PDIs. It has been demonstrated that the well-ordered phase separation behavior is not necessary for the achievement of good mechanical performance.[38] The detailed comparison of the morphologies with different polymer architectures has also been discussed elsewhere.[39] However, the relative positions of these peaks are in general agreement with the AFM images. For instance, MG-29.3-3.0-33.8 exhibits peaks corresponding to a hexagonal morphology, which is consistent with its phase image in AFM (Fig. 3b).

Mechanical properties of PBA-*g*-PMMA graft copolymers

As shown in Fig. 4a, the typical stress *versus* strain curve reveals the exceptional mechanical properties of all-acrylic multigraft superelastomers. It is known that the volume fraction of the two components will affect the mechanical behavior of polyacrylate-based graft copolymers.[21] Herein, the distinct influence of the polymer molecular weight is demonstrated. Several interesting results are found from uniaxial tensile tests on such materials, including: (1) with increasing volume fraction of PMMA, the mechanical strength could be adjusted over a wide range from 1.9 MPa (vol% of PMMA ~10%) to 10.8 MPa (vol% of PMMA ~34%). Meanwhile, the elongation of the material was sacrificed. (2) Interestingly, as compared to our previous study,[21] MG-8.4-3.3-8.6 exhibits much higher stress at break and elongation at break as compared to the previously reported materials with the same structure and similar molecular weight (MG 11.7-5.3-22.2 with ε_B around 450% and σ_B around 0.6 MPa) even though fewer branch points exist in the polymers of this study. The number of branch points has previously been demonstrated to be another key factor that influences mechanical performance.[40] The distinct improvement achieved in the present work can be explained by the molecular weight between chain entanglements, M_e. With M_e (PBA) of 28 kg mol^{-1}, the increase in M_n (PBA) brings more chain entanglements, which in return, helps increase the modulus.[8] (3) The M_e difference between PBA and polyisoprene (M_e: 6.1 kg mol^{-1}) or polybutadiene (M_e: 1.7 kg mol^{-1}) leads to a poorer mechanical performance of polyacrylate TPEs as compared to that of styrenic TPEs.[10] However, surprisingly the combination of high molecular weight and the multigraft architecture endows the synthesized polymers with exceptional elongation at break and tensile strength. All the polymer samples synthesized in this work show better ultimate elongation than PMMA-*b*-PBA-*b*-PMMA

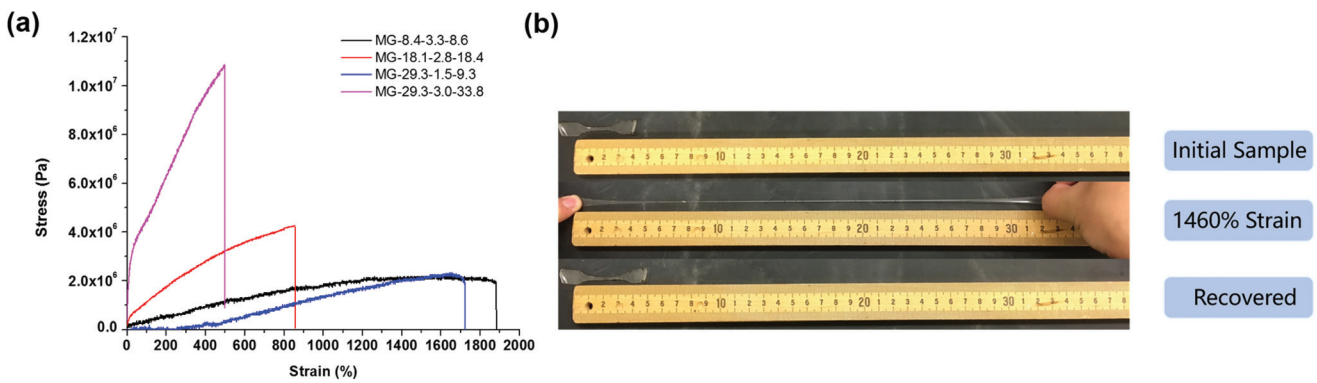

Fig. 4 (a) Stress–strain curves of various PBA-*g*-PMMA samples. (b) Photographs on the hysteresis test of MG-29.3-1.5-9.3. From top to bottom are: initial sample with a gauge length of 16 mm; sample stretched to 250 mm with around 1460% strain; recovered sample with a gauge length of around 18 mm.

triblock copolymers having a similar PMMA content. For example, MG-18.1-2.8-18.4 shows elongation at break of 856%, while similar triblock copolymers with vol% (PMMA) of 22% only exhibited an elongation at break of 545%.[41] Even with the vol% (PMMA) of 33.8%, the elongation at break is still around 500%. (4) With the deformation of such a soft low modulus material, large elongation (~300%) with low stress was observed for MG-29.3-1.5-9.3. The broad PDI indicates the presence of a mixture of multigraft copolymers with different numbers of branches, with the average value of 1.5. The stress at break of 2.0 MPa and strain at break of 1712% are far beyond the performance of commercial PMMA-*b*-PBA-*b*-PMMA triblock copolymers like Arkema's Nanostrength® and with stress lower than 1 MPa and ultimate elongation only around 500%.[42] Moreover, its elongation is even superior to that of commercial styrenic TPEs like Kraton® at 1080%, and comparable to the double tailed PI-*g*-PS multigraft copolymer superelastomers at around 1600%.[18] Thus, all-acrylic superelastomers are produced by synthetic strategies reported in this work.

Another key aspect of superelastomers is their exceptional elastic recovery. As reported by Mays *et al.*, PI-*g*-PS with tetrafunctional branch points exhibits superior recovery with only 40% residual strain after being stretched to 1400% elongation.[40] The hysteresis of the PBA-*g*-PMMA graft copolymer was examined by stretching of the dog-bone specimen, as shown in Fig. 4b. With the initial cross-head separation of around 16 mm, the sample was stretched to 250 mm. The tension was released and the specimen was allowed to return to its original shape, with less than 2 mm residual strain (<15%). In another test, the specimen, with the initial cross-head separation of around 14 mm, was stretched to 1115% elongation twice. It was allowed to return to its original shape, with around 1 mm residual strain each time (7%) (Fig. S3†). For the first time, we report the elongational recovery behavior of all-acrylic TPEs. Due to the lack of previously reported data, we did not attempt to add a quantitative comparison with the corresponding ABA triblocks. However, based on our previous work on styrenic superelastomers, we know that the elastic recovery of all acrylic superelastomers will be far superior to that of linear all-acrylic triblock copolymers.[18,40,42] The greatly improved elastic recovery behavior of multigraft copolymers as compared to linear triblocks is actually a very logical and fully anticipated result. For ABA triblock copolymers the two glassy end blocks can reside in different glassy domains (forming bridges) or in a single glassy domain (forming loops). Only the former contributes to elastic recovery. In contrast, for multigraft copolymers the elastic backbone is much more likely to be tethered to multiple glassy domains, thus resulting in improved elastic recovery.[37,43] The schematic illustration was shown in our previous work and can be found in Fig. S4.† Thus, the excellent elastic recovery of these new all-acrylic graft copolymers is thus demonstrated.

Linear viscoelastic properties of PBA-*g*-PMMA graft copolymers

In addition to DMA, the linear viscoelastic properties of the graft copolymers were measured using a rotational rheometer. As shown in Fig. 5a, the Cole–Cole plot representation gives an overview of the dynamic mechanical spectra at different temperatures without resorting to the Time-Temperature Superposition (TTS) method. Several conclusions can be

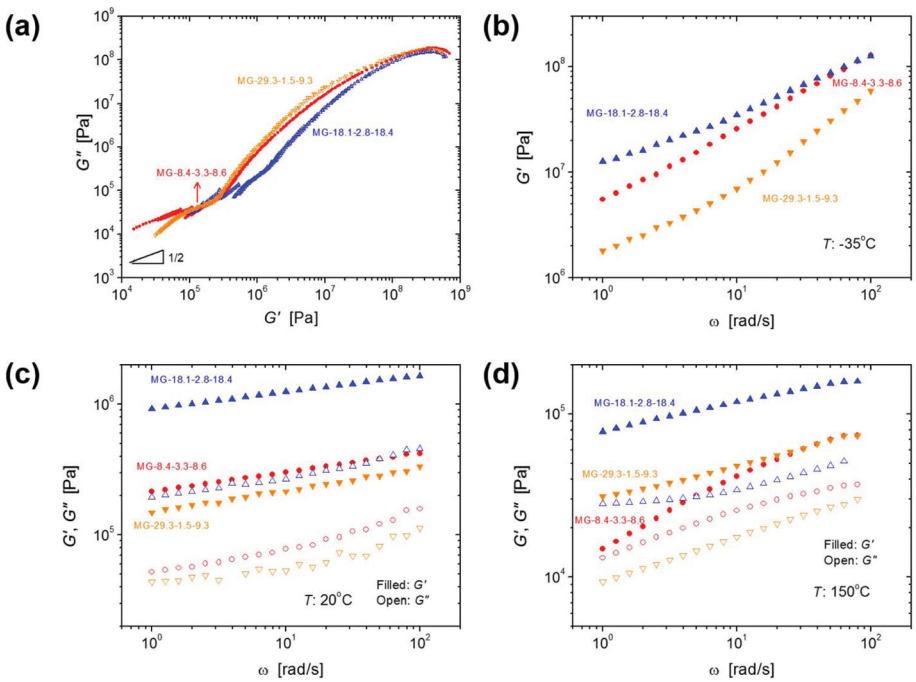

Fig. 5 (a) Cole–Cole plot of various PBA-*g*-PMMA samples. The arrow indicates the level of the plateau modulus. Storage (*G*′) and loss (*G*″) modulus *versus* frequency at representative temperatures including: (b) −35 °C; (c) 20 °C: and (d) 150 °C.

drawn for these graft copolymers: (1) MG-8.4-3.3-8.6 and MG-18.1-2.8-18.4 exhibit thermo-rheological complexity – the failure of TTS. This can be seen from the data collected at intermediate and high temperatures, as they do not collapse onto a single curve. TTS apparently works in MG-29.3-1.5-9.3, due to the relatively low number of branches and low volume fraction of PMMA. (2) All samples display a clear signature of the rubbery plateau at intermediate temperatures, which is classic for thermoplastic elastomers (Fig. 5c). (3) At high temperatures, MG-8.4-3.3-8.6 exhibits liquid-like behavior, due to the relatively weak phase separation in these samples. Moreover, at low temperatures (−35 °C), the mechanical behavior is dominated by T_g. The storage modulus at low frequencies increases with the increase in the PMMA volume fraction (Fig. 5b). At high temperatures, the mechanical behavior is affected by a number of factors, including molecular weight, T_g, the number of branches, and the degree of phase separation. MG-8.4-3.3-8.6 is liquid-like at 150 °C whereas MG-18.1-2.8-18.4 and MG-29.3-1.5-9.3 are still gel-like (Fig. 5d).

Conclusions

In conclusion, a new method to synthesize a graft copolymer of poly(butyl acrylate)-*g*-poly(methyl methacrylate) (PBA-*g*-PMMA) based on a facile grafting through methodology is reported. The initiation system of *sec*-BuLi/PVBA makes it possible to synthesize the PMMA macromonomer in one batch *via* anionic polymerization, with quantitative conversion and short reaction time, making it superior to previously utilized routes. The resulting graft copolymers exhibit microphase separated morphologies. For the first time with all-acrylic block copolymers, the combination of the multi-graft architecture and increased overall molecular weight endow the synthesized copolymers with superelastomeric properties: elongation at break far exceeding that of conventional triblock copolymer polyacrylate TPEs. In addition, their excellent elastic recovery was demonstrated, making these all-acrylic multigraft copolymer TPEs superior to traditional linear triblock type TPEs. Their distinctive mechanical properties offer the potential to expand the range of all-acrylic TPEs, in applications such as thinner surgical gloves and condoms.

Conflicts of interest

Acknowledgements

This work was supported by the U.S. Department of Energy, Office of Science, Basic Energy Sciences, Materials Sciences, and Engineering Division. Part of the synthesis and characterization was conducted at the Center for Nanophase Materials Sciences, which is a DOE Office of Science User Facility. The SAXS research used resources of the Advanced Photon Source, a U.S. Department of Energy (DOE) Office of Science User Facility operated for the DOE Office of Science by Argonne National Laboratory under Contract No. DE-AC02-06CH11357.

Notes and references

1 G. Holden, in *Kirk-Othmer Encyclopedia of Chemical Technology*, John Wiley & Sons, Inc., 2000, DOI: 10.1002/0471238961.2008051808151204.a01.pub2.
2 F. Auriemma and C. De Rosa, *J. Am. Chem. Soc.*, 2003, **125**, 13143–13147.
3 J. Li, J. A. Viveros, M. H. Wrue and M. Anthamatten, *Adv. Mater.*, 2007, **19**, 2851–2855.
4 G. Kraus and K. W. Rollmann, *J. Polym. Sci., Part B: Polym. Phys.*, 1976, **14**, 1133–1148.
5 W. Lu, C. Huang, K. Hong, N.-G. Kang and J. W. Mays, *Macromolecules*, 2016, **49**, 9406–9414.
6 W. Lu, P. Yin, M. Osa, W. Wang, N.-G. Kang, K. Hong and J. W. Mays, *J. Polym. Sci., Part B: Polym. Phys.*, 2017, **55**, 1526–1531.
7 J. G. Drobny, *Handbook of thermoplastic elastomers*, Elsevier, 2014.
8 J. D. Tong and R. Jerôme, *Polymer*, 2000, **41**, 2499–2510.
9 W. Lu, Y. Wang, W. Wang, S. Cheng, J. Zhu, Y. Xu, K. Hong, N.-G. Kang and J. Mays, *Polym. Chem.*, 2017, **8**, 5741–5748.
10 J.-D. Tong and R. Jerôme, *Macromolecules*, 2000, **33**, 1479–1481.
11 R. C. Coffin, Y. Schneider, E. J. Kramer and G. C. Bazan, *J. Am. Chem. Soc.*, 2010, **132**, 13869–13878.
12 D. J. Pochan, S. P. Gido, S. Pispas, J. W. Mays, A. J. Ryan, J. P. A. Fairclough, I. W. Hamley and N. J. Terrill, *Macromolecules*, 1996, **29**, 5091–5098.
13 H. K. Choi, A. Nunns, X. Y. Sun, I. Manners and C. A. Ross, *Adv. Mater.*, 2014, **26**, 2474–2479.
14 W. Wang, W. Lu, N.-G. Kang, J. Mays and K. Hong, in *Elastomers*, ed. N. Cankaya, InTech, Rijeka, 2017, ch. 05, DOI: DOI: 10.5772/intechopen.68586.
15 J. W. Mays, D. Uhrig, S. Gido, Y. Zhu, R. Weidisch, H. Iatrou, N. Hadjichristidis, K. Hong, F. Beyer, R. Lach and M. Buschnakowski, *Macromol. Symp.*, 2004, **215**, 111–126.
16 J. Mijović, M. Sun, S. Pejanović and J. W. Mays, *Macromolecules*, 2003, **36**, 7640–7651.
17 D. Uhrig, R. Schlegel, R. Weidisch and J. Mays, *Eur. Polym. J.*, 2011, **47**, 560–568.
18 Y. Zhu, E. Burgaz, S. P. Gido, U. Staudinger, R. Weidisch, D. Uhrig and J. W. Mays, *Macromolecules*, 2006, **39**, 4428–4436.
19 D. Uhrig and J. Mays, *Polym. Chem.*, 2011, **2**, 69–76.
20 S. Ito, R. Goseki, T. Ishizone and A. Hirao, *Polym. Chem.*, 2014, **5**, 5523–5534.
21 A. Goodwin, W. Wang, N.-G. Kang, Y. Wang, K. Hong and J. Mays, *Ind. Eng. Chem. Res.*, 2015, **54**, 9566–9576.
22 W. Radke, S. Roos, H. M. Stein and A. H. E. Müller, *Macromol. Symp.*, 1996, **101**, 19–27.

23 S. G. Roos, A. H. Müller and K. Matyjaszewski, *Macromolecules*, 1999, **32**, 8331–8335.
24 W. Wang, W. Wang, X. Lu, S. Bobade, J. Chen, N.-G. Kang, Q. Zhang and J. Mays, *Macromolecules*, 2014, **47**, 7284–7295.
25 F. Zeng, Y. Shen and S. Zhu, *Macromol. Rapid Commun.*, 2001, **22**, 1399–1404.
26 N. Hadjichristidis, H. Iatrou, S. Pispas and M. Pitsikalis, *J. Polym. Sci., Part A: Polym. Chem.*, 2000, **38**, 3211–3234.
27 D. Uhrig and J. W. Mays, *J. Polym. Sci., Part A: Polym. Chem.*, 2005, **43**, 6179–6222.
28 J. T. Lai, D. Filla and R. Shea, *Macromolecules*, 2002, **35**, 6754–6756.
29 A. Seki, F. Ishiwata, Y. Takizawa and M. Asami, *Tetrahedron*, 2004, **60**, 5001–5011.
30 H. Gilman, A. H. Haubein and H. Hartzfeld, *J. Org. Chem.*, 1954, **19**, 1034–1040.
31 R. Fayt, R. Forte, C. Jacobs, R. Jerome, T. Ouhadi, P. Teyssie and S. K. Varshney, *Macromolecules*, 1987, **20**, 1442–1444.
32 F. Ziaee and M. Nekoomanesh, *Polymer*, 1998, **39**, 203–207.
33 H. Iatrou, J. W. Mays and N. Hadjichristidis, *Macromolecules*, 1998, **31**, 6697–6701.
34 D. Uhrig and J. W. Mays, *Macromolecules*, 2002, **35**, 7182–7190.
35 S. N. Magonov, V. Elings and M. H. Whangbo, *Surf. Sci.*, 1997, **375**, L385–L391.
36 F. S. Bates and G. H. Fredrickson, *Annu. Rev. Phys. Chem.*, 1990, **41**, 525–557.
37 Y. Duan, M. Thunga, R. Schlegel, K. Schneider, E. Rettler, R. Weidisch, H. W. Siesler, M. Stamm, J. W. Mays and N. Hadjichristidis, *Macromolecules*, 2009, **42**, 4155–4164.
38 J. W. Mays, D. Uhrig, S. Gido, Y. Zhu, R. Weidisch, H. Iatrou, N. Hadjichristidis, K. Hong, F. Beyer and R. Lach, 2004.
39 H. Wang, W. Lu, W. Wang, P. N. Shah, K. Misichronis, N.-G. Kang and J. W. Mays, *Macromol. Chem. Phys.*1700254, DOI: 10.1002/macp.201700254.
40 U. Staudinger, R. Weidisch, Y. Zhu, S. Gido, D. Uhrig, J. Mays, H. Iatrou and N. Hadjichristidis, 2006.
41 C. Moineau, M. Minet, P. Teyssié and R. Jérôme, *Macromolecules*, 1999, **32**, 8277–8282.
42 J.-M. Boutillier, J.-P. Disson, M. Havel, R. Inoubli, S. Magnet, C. Laurichesse and D. Lebouvier, 2013.
43 Y. Duan, E. Rettler, K. Schneider, R. Schlegel, M. Thunga, R. Weidisch, H. W. Siesler, M. Stamm, J. W. Mays and N. Hadjichristidis, *Macromolecules*, 2008, **41**, 4565–4568.